

## PAPER

View Article Online  
View Journal | View Issue



Cite this: *Environ. Sci.: Adv.*, 2023, 2, 529

# Insights into the rare earth element potential of coal combustion by-products from western Canada†

Brendan A. Bishop,<sup>a</sup> Karthik Ramachandran Shivakumar,<sup>b</sup> Daniel S. Alessi<sup>b</sup> and Leslie J. Robbins<sup>a</sup>

Rare earth elements (REE) have been designated as critical minerals by several nations and demand is anticipated to increase as a result of their requirement in clean energy technologies. It has been noted that the current supply of REE may be unable to satisfy this demand, therefore it is becoming increasingly important to find new sources of these metals. Coal combustion by-products (CCBs), including fly and bottom ashes, have emerged potential sources of REE due to their wide availability and environmental and economic incentives for reuse. However, the geochemical composition of the CCBs governs the effectiveness of a given extraction process, therefore they require characterization prior to the development of an efficient, low-cost method for REE recovery. In this study, CCBs from Alberta and Saskatchewan, Canada were investigated using bulk digestions, acid leaching, and sequential extractions to assess western Canadian CCBs as a source of REE. The Ca-rich CCBs from Poplar River contained the highest concentration of REE and nearly 100% of the REE were recovered using acid leaching. Conversely, REE recovery in acid leaches in Si-rich samples from Boundary Dam, Shand, and Alberta ranged from 3 to 65%. Sequential extractions indicated that the REE are primarily hosted in the residual, aluminosilicate phase in all samples consistent with previous studies. Geochemical data for the CCBs in this study were combined with existing data from around the world and subjected to unsupervised machine learning algorithms to assess for potential indicators of REE enrichment. The results indicate REE are correlated with Ti, Si, Zr, Al, and Th and are likely associated with clay and/or detrital minerals. The recovery of REE from CCBs could provide a near-term, environmentally friendly source of critical minerals while addressing the United Nations Sustainable Development Goals 7, 12, and 13.

Received 8th December 2022  
Accepted 8th February 2023

DOI: 10.1039/d2va00310d

rsc.li/esadvances

## Environmental significance

Rare earth elements (REE) are crucial in clean energy technologies; however, due to projected shortages, numerous environmental concerns regarding increased production, and domestic supply chain constraints, there is recent interest in recovering REE from waste streams including coal combustion by-products (CCBs). Here, the recovery of REE from CCBs in western Canada is investigated using an integrated geochemical and machine learning study which indicates they could be a domestic, near-term source of REE which can alleviate supply chain concerns and provide materials crucial for the energy transition. Since only a small amount of CCBs are reused, recovery of REE has the added benefit of remediation since their long-term storage can lead to the release of contaminants into the environment.

## Introduction

The rare earth elements (REE), comprising the 15 lanthanide elements as well as Sc and Y, are coveted for their unique physical, optical, magnetic, and chemical properties which make them vital in clean energy, consumer electronic, and

defense technologies.<sup>1,2</sup> Demand for REE is anticipated to increase substantially driven by the global transition to a clean energy economy,<sup>3,4</sup> which will require both an increase in primary REE production and the development of new sources.<sup>2</sup> The largest, single use of REE is in permanent magnets which are used in clean energy technologies including electric vehicles and wind turbines, which require neodymium (Nd), and to a lesser extent, praseodymium (Pr) and dysprosium (Dy). The incorporation of these magnets into clean energy technologies is expected to be a significant driver of the anticipated increase in demand.<sup>4</sup> However, the global supply chain is dominated by China, which produces ~60% of the global share<sup>5</sup> and processes

<sup>a</sup>Department of Geology, University of Regina, 3737 Wascana Parkway, Regina, SK, S4S 0A2, Canada. E-mail: bab495@uregina.ca

<sup>b</sup>Department of Earth and Atmospheric Sciences, University of Alberta, 1-26 Earth Sciences Building, Edmonton, AB, T6G 2E3, Canada

† Electronic supplementary information (ESI) available. See DOI: <https://doi.org/10.1039/d2va00310d>



an estimated 86% of all REE.<sup>6</sup> This had led to concerns that the global supply chain could be disrupted in a manner similar to the REE crisis of the early 2010s.<sup>7</sup> Given their economic importance and inherent supply chain concerns, the governments of Canada, Australia, the United States, and the European Union have each classified REE as critical metals.

Although REE are required for the energy transition, there are a number of concerns regarding both increased production and the development of new mining projects. The extraction of REE from primary deposits is linked to environmental and social issues including water resource contamination, greenhouse gas emissions, land depletion, radioactive tailings production, effects on Indigenous groups, and human health concerns.<sup>8</sup> In addition, REE are among the most energy intensive metals to produce on a per mass basis,<sup>9</sup> so although technologies containing REE are critical in reducing energy emissions, paradoxically the energy required to extract these metals has the potential to further exacerbate climate change. Using system dynamics modelling incorporating life cycle assessment, Golroudbary<sup>10</sup> found that rapid development of green energy technologies could lead to an unsustainable consumption of REE. In light of these concerns, there has been substantial interest in extracting REE from alternative sources including recycling,<sup>3,11,12</sup> acid mine drainage systems,<sup>13–15</sup> mining waste,<sup>16,17</sup> geothermal and oilfield brines,<sup>18,19</sup> and coal combustion by-products (CCBs).<sup>20–23</sup>

Among these, coal combustion by-products are emerging as a promising source of REE based on several factors including: (i) availability as a low-cost waste product with strong incentives for reuse due to environmental liabilities of ash storage; (ii) a reduced requirement for excavation or beneficiation thereby eliminating the most energy intensive processes involved in REE mining; and (iii) the elimination of radioactive tailings.<sup>23,24</sup> During the combustion process, REE are immobile and can be enriched up to 30 times in the ashes relative to the source coal,<sup>25,26</sup> with the geochemical composition of the coal, combustion conditions in the boiler, carbon content, and particle size controlling the REE abundance.<sup>27</sup> Several studies have investigated REE abundances in CCBs from a number of countries including: Canada,<sup>28</sup> the United States,<sup>23,25,29,30</sup> Brazil,<sup>31</sup> China,<sup>32,33</sup> the United Kingdom,<sup>21</sup> South Africa,<sup>34</sup> and Poland.<sup>20,21</sup> Yet, because of the variability in source coal geochemistry and combustion conditions, geochemical characterization of the CCBs from each plant is required to develop effective extraction processes,<sup>23</sup> and although several studies have assessed the potential for REE recovery from CCBs from around the world, those from Canada have yet to be systematically studied.

This research presents the first in-depth investigation of REE in CCBs from Canada, characterizing ashes from coal fired power plants in Alberta and Saskatchewan. Bulk geochemistry including REE concentrations were determined by total digestion, while the extraction potential was assessed using acid leach experiments and sequential extractions. Compositional data analysis and unsupervised machine learning algorithms were used to compare the geochemistry of the investigated CCBs with data from previous studies to reveal potential

geochemical associations and elemental indicators of REE enrichment. Characterization of CCBs is critical for understanding the potential for REE extractability and, in turn, designing effective recovery strategies which may vary based on power plant operating conditions and the geological and depositional history of the coal deposit. Developing new sources of REE is critical to support the production of technologies required to meet climate change goals, and “mining” them from coal waste has the added benefit of turning a waste stream into an economic asset while simultaneously remediating an environmental liability. Further, this can address the United Nations (UN) Sustainable Development Goals (SDG) 7 (Affordable and Clean Energy), 12 (Responsible Consumption and Production), and 13 (Climate Action).

## Materials and methods

### Materials

Coal fly ash (FA) and bottom ash (BA) samples were provided by utility companies for three coal-fired power stations in Saskatchewan and one in Alberta, all of which source their coal from the Western Canada Sedimentary Basin. Samples from Saskatchewan were provided for the Poplar River (PR), Boundary Dam (BD), and Shand (SND) power stations, the three coal-fired power stations in the province. Coal for the Poplar River station is sourced from the Poplar River mine, while coal for the Boundary Dam and Shand stations comes from the Estevan mine. These power stations burn lignite coal from the Paleocene Ravenscrag Formation of the Williston sub-basin which is stratigraphically equivalent to the Fort Union Formation of the Powder River Basin.<sup>35</sup> Samples from Alberta were provided for a single generating station with two generators, a lower temperature boiler (AB12) and a higher temperature boiler (AB3) which burn sub-bituminous coal from the upper Cretaceous-Paleocene Scollard Formation of the Alberta sub-basin. In total, five sets of CCBs were analyzed in this study.

### Bulk digestions

Elemental abundances were determined utilizing a lithium borate fusion digestion followed by inductively coupled plasma mass spectrometry (ICP-MS) by Bureau Veritas, Vancouver, BC (LF200 method). In-house certified reference materials (STD SO-19) were analyzed in tandem to monitor analytical precision and reproducibility. Additional details, including geochemical data for the Saskatchewan samples, can be found in Bishop *et al.*<sup>28</sup>

### Acid leaches

Acid leach experiments were performed to assess the ability of acid to liberate REE from the CCBs. Conditions for acid leaches were based on the optimal conditions determined by Cao *et al.*<sup>36</sup> of a 1 : 10 sample : acid ratio in 3 M HCl and a two-hour contact time. Here, 0.5 g of sample was suspended in 5 mL of 3 M HCl in PFA vials for two hours at room temperature (20–22 °C) with periodic agitation. Solutions were then filtered through 0.2 µm nylon filters and diluted in 2% HNO<sub>3</sub> prior to ICP-MS analysis on an Agilent 8800 ICP-MS/MS at the Environmental



Geochemistry Lab, University Alberta, using a 2 parts per million (ppm) indium internal standard to correct for instrument drift. Each acid leach was performed in duplicate with the average being reported.

### Sequential extractions

Sequential extractions were performed in duplicate following the methods of von Gunten *et al.*,<sup>37</sup> based on Tessier *et al.*,<sup>38</sup> to elucidate the mode of occurrence of REE in the CCBs. This method differentiates between five fractions: (1) exchangeable; (2) carbonate-bound (acid soluble); (3) Fe–Mn-oxide bound (reducible); (4) organic matter and sulfide bound (oxidizable); and (5) residual. Sequential extractions were performed as follows: for the exchangeable fraction, 1 g of sample was suspended in 8 mL of 0.5 M magnesium chloride and rotated for 1 h; the carbonate bound fraction was determined by suspending the remaining solids in 8 mL of 1 M sodium acetate adjusted to pH 5 with acetic acid and rotated for 5 h; the reducible fraction was determined by exposing the solids to 20 mL of 0.04 M hydroxyl ammonium hydrochloride for 6 h at 96 °C with hourly agitation; and finally, the oxidizable fraction was determined following the addition of 3 mL of 0.02 M nitric acid and 5 mL of 30% hydrogen peroxide solution placed in an oven at 85 °C for 2 h followed by the addition of 3 mL hydrogen peroxide adjusted to pH 2 which was allowed to react for a further 3 h. The solution was then cooled to room temperature and allowed to react with 4 mL ultrapure water and 5 mL of 3.2 M ammonium acetate in 20% V/V nitric acid for 30 min with continuous agitation. Between each step, the samples were centrifuged at 10 000 g for 10 min, the resulting supernatant was filtered through 0.2 µm nylon filters, diluted in 2% nitric acid and analyzed following the same approach as the acid leach experiments. The solids were rinsed with 18.1 MΩ cm water for 10 minutes and centrifuged prior to the next step. The residual fraction was determined by subtracting the concentrations from steps 1–4 from the total concentration of the analyzed element.

### Data acquisition and analysis

Geochemical data from previous CCB studies<sup>20,21,23,24,26,27,30,34,39–63</sup> was compiled to compare REE contents of western Canadian CCBs with other localities and to identify elemental indicators of REE enrichment using unsupervised machine learning. Where available, major oxide, trace element, REE, coal rank, country, and sedimentary basin information was compiled for FA and BA samples from around the world. In studies where time sequence samples were taken, the first sample was used. For studies which sampled multiple electrostatic (ESP) rows, the composition of the fly ash from the first row was taken since Hower *et al.*<sup>64</sup> indicated the first row captures 80% of the fly ash. Since multivariate data analysis can not be performed on censored data, such as data points which are below the detection limit, when an individual REE was below the detection limit, the value was set as half the detection limit as defined in each study. In cases where there was no detection limit reported in the study, the value was set to zero. To avoid performing data analysis where values of zero were present, the sum of the REE

was used. Oxide weight percent concentrations were converted to elemental ppm concentrations. When sample context (*i.e.*, coal rank) was missing, efforts were made to add this information based on existing literature. The complete dataset including the geochemical data and sample context information (location, coal rank, ash type, reference) is in Table SI1.† Table SI2† contains the geochemical data, including major element, REE, and select trace elements, for the correlation analysis, principal component analysis (PCA), and cluster analysis. Elements were selected in order to strike a balance between maximizing the number of variables for which data existed and the number of observations. All statistical and data analysis was performed using the R programming language,<sup>65</sup> the correlation matrix was created using the corrgram package,<sup>66</sup> the PCA and cluster analysis visualization was completed with the factoextra package<sup>67</sup> using the Viridis colour palette.<sup>68</sup>

## Results and discussion

### REE abundances in western canadian CCBs

Rare earth elements have been classified by IUPAC into the light REE (LREE; La to Gd) and heavy REE (HREE; Tb to Lu, and Y) on the basis of the configuration of their 4f electron shells. In addition, REE have been categorized based on their demand into critical REE (CREE; Nd, Eu, Tb, Dy, Y, and Er), uncritical REE (UREE; La, Pr, Sm, and Gd), and excessive REE (UREE; Ce, Ho, Tm, Yb, and Lu),<sup>69</sup> however this classification is somewhat subjective and transient depending on global supply and demand.<sup>70</sup> As such, in addition to total REE (TREE) and CREE, Nd concentrations will also be highlighted since its demand is anticipated to have the greatest increase due to incorporation in permanent magnets and because TREE content can be influenced by anomalous behaviour of less valuable elements including La, Ce, Eu, Gd, and Y. Seredin and Dai<sup>69</sup> have defined the outlook coefficient as the ratio of the relative amount of the CREE to the EREE as  $C_{\text{outlook}} = (\text{CREE}/\text{TREE})/(\text{EERE}/\text{TREE})$ . The REE data – including LREE, HREE, TREE, CREE, UREE, EREE, and  $C_{\text{outlook}}$  – for this study is presented in Table 1, while the major and trace element data is provided in Table 2.

Total REE concentrations of the samples range from 258.9 to 320.5 ppm with an average of 285 ppm, lower than the average of 399.5 ppm from Powder River Basin CCBs,<sup>29</sup> as well as the median (326 ppm) and mean (368 ppm) from the compiled global dataset (Table SI1). Neodymium concentrations in the western Canada samples are also slightly lower than the global CCB average. The average CREE content is 102 ppm, while the percent critical REE ranges from 32.5 to 38.7%, with an average of 36%. This is consistent with the mean value of 37% for the CCBs from coal sourced from the Powder River Basin<sup>29</sup> and 37% from the compiled dataset. The  $C_{\text{outlook}}$  for these samples varies from 0.85 to 1.11. Since the %CREE is >30% and  $C_{\text{outlook}}$  is >0.7 for all samples, they are considered “promising” sources of REE based on Seredin and Dai.<sup>69</sup> However, the combined economics of REE concentration and extraction will ultimately determine whether these CCBs can be a potential REE source.



**Table 1** Rare earth element data (in ppm) for Saskatchewan and Alberta CCBs. FA – fly ash, BA – bottom ash, AB12 – Alberta lower temperature boiler, AB3 – higher temperature boiler, BD – Boundary Dam, PR – Poplar River, SND – Shand

Element	AB12BA	AB12FA	AB3BA	AB3FA	BDBA	BDFA	PRBA	PRFA	SNDBA	SNDFA
La	46.7	51.8	49.9	55.2	53.4	49.9	59.1	64.5	49.4	47
Ce	89.1	96.6	94.5	104.4	99.8	91	100.8	116.1	88.3	87.2
Pr	10.34	11.75	11.12	12.21	11.49	10.47	11.49	12.64	10.43	10.14
Nd	38.9	45.5	42.1	45.4	43.2	39.3	41.8	46.3	38.6	37.1
Sm	7.55	8.56	7.75	8.37	8.29	6.95	7.7	8.6	7.52	7.15
Eu	1.53	1.75	1.55	1.52	1.69	1.43	1.33	1.52	1.35	1.36
Gd	7.11	8.09	7.45	7.81	8.78	7.03	6.84	7.96	7.38	7.11
Tb	1.06	1.27	1.14	1.18	1.41	1.07	1.09	1.21	1.18	1.12
Dy	6.46	7.62	6.77	6.88	8.68	6.32	6.77	6.88	7.39	7
Y	39.9	48.5	43.1	44.3	59.4	43.9	41.5	44.2	48.5	45.5
Ho	1.36	1.61	1.43	1.47	1.95	1.38	1.33	1.43	1.56	1.47
Er	3.97	4.92	4.41	4.38	5.91	4.03	3.88	4.13	4.82	4.43
Tm	0.55	0.67	0.64	0.62	0.84	0.58	0.57	0.6	0.68	0.61
Yb	3.76	4.54	4.24	4.11	5.31	3.86	3.78	3.79	4.38	4.12
Lu	0.59	0.76	0.68	0.67	0.86	0.59	0.56	0.59	0.65	0.63
LREE	201.23	224.05	214.37	234.91	226.65	206.08	229.06	257.62	202.98	197.06
HREE	57.65	69.89	62.41	63.61	84.36	61.73	59.48	62.83	69.16	64.88
TREE	258.9	293.9	276.8	298.5	311	267.8	288.5	320.5	272.1	261.9
CREE	91.8	109.6	99.1	103.7	120.3	96.1	96.4	104.2	101.8	96.5
UREE	71.7	80.2	76.2	83.6	82	74.4	85.1	93.7	74.7	71.4
EREE	95.4	104.2	101.5	111.3	108.8	97.4	107	122.5	95.6	94
pCritical	35.5	37.3	35.8	34.7	38.7	35.9	33.4	32.5	37.4	36.8
C <sub>outlook</sub>	0.96	1.05	0.98	0.93	1.11	0.99	0.9	0.85	1.07	1.03

Although the FAs are all technically classified as Type F ash based on their composition, the CCBs from each location show distinct variations in their overall geochemistry. The Poplar

River samples are characterized by the highest concentrations of TREE, Nd, CaO, Al<sub>2</sub>O<sub>3</sub>, MgO, Ga, Th, U, and W and lowest levels of SiO<sub>2</sub>, Na<sub>2</sub>O, K<sub>2</sub>O, Co, and Ni and proportion of CREE.

**Table 2** Major and trace element data for Saskatchewan and Alberta CCBs. FA – fly ash, BA – bottom ash, AB12 – Alberta lower temperature boiler, AB3 – higher temperature boiler, BD – Boundary Dam, PR – Poplar River, SND – Shand

Sample	SiO <sub>2</sub> (wt%)	Al <sub>2</sub> O <sub>3</sub> (wt%)	Fe <sub>2</sub> O <sub>3</sub> (wt%)	MgO (wt%)	CaO (wt%)	Na <sub>2</sub> O (wt%)	K <sub>2</sub> O (wt%)	TiO <sub>2</sub> (wt%)	P <sub>2</sub> O <sub>5</sub> (wt%)	MnO (wt%)	Cr <sub>2</sub> O <sub>3</sub> (wt%)	Ba (ppm)	Ni (ppm)	Sc (ppm)	Be (ppm)
AB12BA	62.56	20.44	5.45	1.25	5.12	1.94	1.64	0.63	0.04	0.08	0.008	2048	27	14	3
AB12FA	59.76	21.21	4.49	1.4	6.33	2.58	1.65	0.69	0.06	0.04	0.013	2639	42	17	6
AB3BA	60.24	19.81	5.95	1.34	6.79	2.17	1.39	0.63	0.04	0.08	0.007	2437	29	14	2
AB3FA	52.81	20.61	4.06	1.48	13.18	2.22	1.21	0.66	0.08	0.05	0.008	3375	39	15	5
BDBA	53.09	18.7	4.89	3.06	11.4	4.56	1.3	0.8	0.4	0.02	0.008	6174	42	17	7
BDFA	54.28	18.91	4.85	3.28	8.35	5.28	2.09	0.67	0.36	0.02	0.011	5047	34	15	7
PRBA	39.41	22.88	10.95	5.77	17.2	0.21	0.61	0.73	0.03	0.06	0.004	3824	10	12	5
PRFA	39.58	26.64	4.76	5.82	18.58	0.35	0.97	0.69	0.06	0.07	0.008	3708	10	14	6
SNDBA	53.57	18.77	4.82	2.83	9.05	3.93	1.76	0.78	0.35	0.02	0.009	5687	35	16	10
SNDFA	53.65	19.26	4.21	2.8	8.16	5.89	1.89	0.76	0.34	0.02	0.009	5169	33	15	7

Sample	Co (ppm)	Cs (ppm)	Ga (ppm)	Hf (ppm)	Nb (ppm)	Rb (ppm)	Sn (ppm)	Sr (ppm)	Ta (ppm)	Th (ppm)	U (ppm)	V (ppm)	W (ppm)	Zr (ppm)
AB12BA	11.1	5.3	12.1	6.6	14.5	61.1	0.5	613.1	1.1	17.3	5.8	91	1.3	249.2
AB12FA	14.8	5.6	27.5	7.7	18.6	64.6	4	804.3	1.2	18.5	7.9	127	2.9	280.6
AB3BA	12.7	3.9	14.8	7.6	17.3	52.7	1	798.9	1.1	17.9	6.7	91	2.1	287.9
AB3FA	13.4	4.2	26.1	7.1	17.1	45.9	3	928.1	1.1	20.4	8.5	98	3.2	259.7
BDBA	13.2	4.5	19.2	8.9	23.4	53.1	2	3262.5	1.7	22.2	12.8	111	5.5	356.2
BDFA	11.7	8.9	30.2	5.9	18.1	91.5	4	2411.6	1.2	17.8	12.5	143	5	228.8
PRBA	4.7	1.8	20.4	9.9	23.8	20.6	3	981	1.9	24.1	13.4	49	6.5	353.6
PRFA	5.1	3.7	65.5	7.5	20.4	35.8	10	1167.5	1.9	29	19.6	76	8.6	257
SNDBA	13.9	6.2	18.6	8.3	20.8	71.5	2	2651.1	1.5	20.6	11.1	120	3.9	303.5
SNDFA	13.2	6.9	29.7	7	19.9	75.3	4	2376.9	1.4	20.7	9.7	118	4.5	272.2



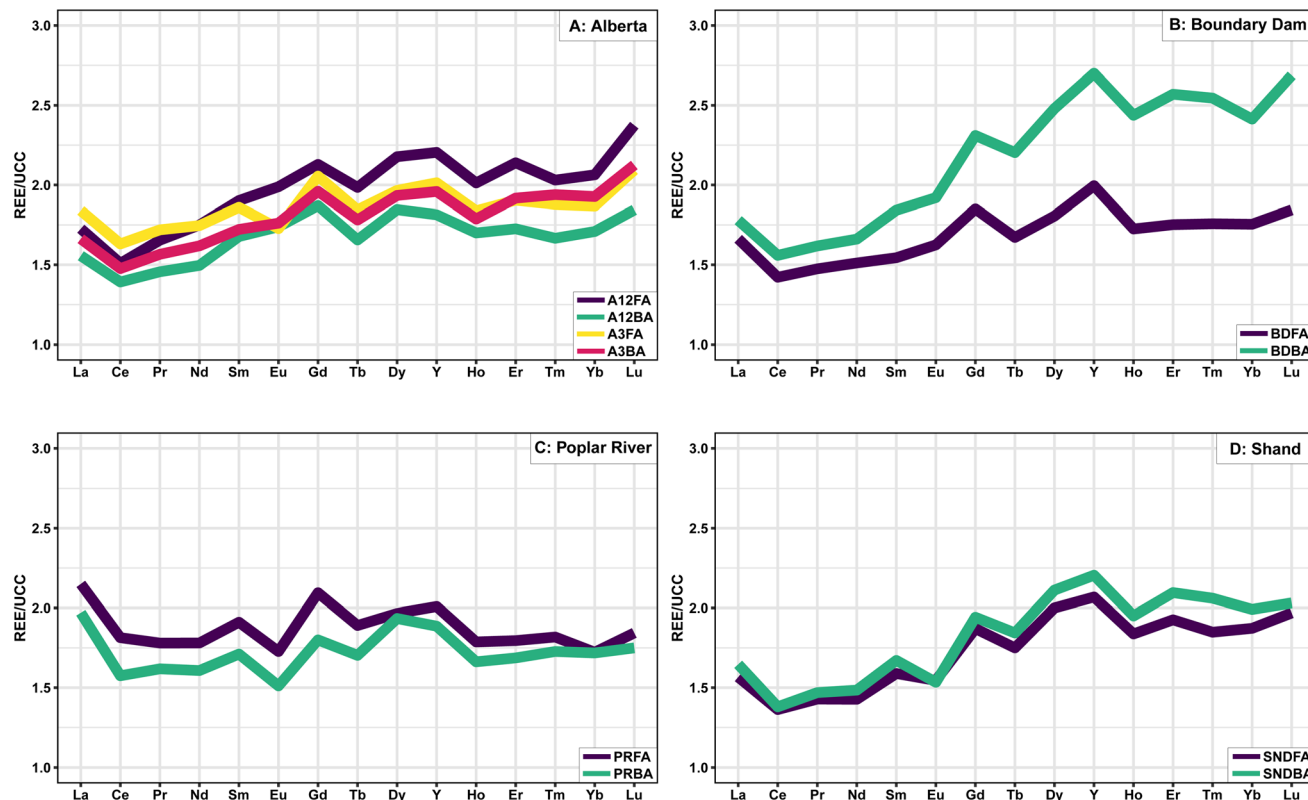


Fig. 1 Spider plot of UCC normalized REE data from each of the four plants. Green (red AB3) = BA, Purple (yellow AB3) = FA.

They are generally enriched in alkaline earth elements and are similar to CCBs derived from Powder River Basin coals.<sup>71</sup> Conversely, the samples from the plant in Alberta typically have the highest SiO<sub>2</sub> and MnO concentrations and the lowest alkaline earth (CaO, MgO, Ba, Be, and Sr), TiO<sub>2</sub>, Nb, U, V, and W concentrations. The Boundary Dam and Shand samples, which both receive coal from the same mine, contain the highest Na<sub>2</sub>O, K<sub>2</sub>O, TiO<sub>2</sub>, Ba, Be, Rb, and Sr and the lowest Al<sub>2</sub>O<sub>3</sub> concentrations. The Alberta, Boundary Dam, and Shand ashes have a somewhat similar composition to CCBs from the combustion of Appalachian Basin coals.

The natural abundance of REE follows the Oddo–Harkins rule, where elements with even numbers are more abundant than elements with odd numbers, and lighter elements are typically more abundant than heavy elements, which leads to characteristic zigzag shapes on abundance diagrams.<sup>72</sup> Normalization to reference materials eliminates this shape and allows for a more straightforward comparison of REE abundances between samples, as well as the identification of anomalous REE behaviour which may yield insights into a sample's geological history.<sup>73</sup> Coal and CCBs are typically normalized to the Upper Continental Crust (UCC)<sup>74</sup> since the ash is derived from the inorganic minerals in the coal which have a similar composition to the bulk continental crust.<sup>72</sup> Spider plots of UCC normalized REE data are presented in Fig. 1.

The fly and bottom ash samples generally show similar normalized trends; however, the Boundary Dam BA is more

enriched in HREE relative to the FA, consistent with Powder River Basin CCBs.<sup>24</sup> Differences between samples from the two units at the Alberta plant are minimal, although the AB12 BA is more enriched in HREE.

Typically, REE behave coherently during geological processes; although there are some processes that may lead to certain REE being fractionated, relative to the others, due to redox changes or differences in the stability of aqueous complexes.<sup>72</sup> Anomalies have been calculated based on Bolhar *et al.*<sup>75</sup> for La, Ce, Gd, and Y (eqn (1)–(4)) and Bau and Dulski<sup>73</sup> for Eu (eqn (5)):

$$\text{La}_N/\text{La}_N^* = \text{La}_N/(3\text{Pr}_N - 2\text{Nd}_N) \quad (1)$$

$$\text{Ce}_N/\text{Ce}_N^* = \text{Ce}_N/(2\text{Pr}_N - 1\text{Nd}_N) \quad (2)$$

Table 3 Calculated REE anomalies for CCB samples

Sample	La/La*	Ce/Ce*	Eu/Eu*	Gd/Gd*	Y <sub>N</sub> /Ho <sub>N</sub>	Pr <sub>N</sub> /Yb <sub>N</sub>
AB12BA	1.13	0.98	1.04	1.28	1.07	0.85
AB12FA	1.18	0.97	1.03	1.19	1.10	0.80
AB3BA	1.14	0.98	1.01	1.20	1.10	0.81
AB3FA	1.10	0.96	0.93	1.19	1.10	0.92
BDFA	1.16	0.99	0.98	1.20	1.11	0.67
BDFA	1.19	0.99	1.02	1.20	1.16	0.84
PRBA	1.20	0.97	0.88	1.22	1.13	0.94
PRFA	1.21	1.02	0.91	1.15	1.12	1.03
SNDBA	1.15	0.95	0.89	1.23	1.13	0.74
SNDBA	1.10	0.95	0.94	1.25	1.13	0.76



$$\text{Gd}_\text{N}/\text{Gd}_\text{N}^* = \text{Gd}_\text{N}/(2\text{Tb}_\text{N} - 1\text{Dy}_\text{N}) \quad (3)$$

$$\text{Y}_\text{N}/\text{Ho}_\text{N} \quad (4)$$

$$\text{Eu}_\text{N}/\text{Eu}_\text{N}^* = \text{Eu}_\text{N}/(0.67\text{Sm}_\text{N} - 0.33\text{b}_\text{N}) \quad (5)$$

where the subscript N indicates the UCC normalized value for the respective element. All samples are characterized by minor positive La, Gd, and Y anomalies, while the Poplar River and Shand samples display negative Eu anomalies (Table 3).

Seredin and Dai<sup>69</sup> described three enrichment patterns in coals including LREE-( $\text{La}_\text{N}/\text{Lu}_\text{N} > 1$ ), MREE-( $\text{La}_\text{N}/\text{Sm}_\text{N} < 1$ ,  $\text{Gd}_\text{N}/\text{Lu}_\text{N} > 1$ ), and HREE-( $\text{La}_\text{N}/\text{Lu}_\text{N} < 1$ ) enriched. Based on this classification, the Poplar River samples are LREE enriched; the Boundary Dam, Shand, AB3, and AB12 FA samples are HREE enriched; and the AB12 BA sample is MREE enriched. Lanthanum anomalies may result from either unusually high stability in fluids related to the absence of the 4f electron<sup>76</sup> or biological processes.<sup>77</sup> As a result, the determination of LREE enrichment may be better calculated using the ratio of  $\text{Pr}_\text{N}/\text{Lu}_\text{N}$  as proposed by Bolhar *et al.*<sup>75</sup> since Pr does not fractionate relative to the other REE. Based on this more suitable method, the Poplar River samples would also be considered HREE enriched.

### Acid leaching

Although some CCBs can contain economic abundances of REE, their extraction and recovery remain a significant obstacle. The first step in the recovery of REE from CCBs typically involves acid leaching to release the REE; however, uncertainty remains surrounding its effectiveness, which in part may depend on ash characteristics.<sup>71</sup> Accordingly, previous studies have investigated both direct leaching, where no pre-treatment of the CCBs is performed, and indirect leaching, where the CCBs are chemically or physically treated prior to acid leaching, as well as the impacts of different acids, lixiviants, alkaline treatments, and/or experimental conditions on leaching efficiency.<sup>36,71,78,79</sup> Leaching results presented here include the percent LREE,

HREE, and TREE released from each CCB following leaching by 3 M HCl (Fig. 2), as well as the major and trace metals (Fig. S1†).

The Poplar River FA sample had the highest leaching efficiency of REE at >97%, followed by the Boundary Dam, Shand, and Alberta FA samples. Correspondingly, the Poplar River FA samples also had the highest leaching of trace metals including Ti, V, Co, Ni, Ga, Sr, Zr, Th, and U. The high leaching efficiency of the Poplar River ashes is likely attributed to the increased concentrations of Ca, likely present as  $\text{CaCO}_3$  based on the sequential extractions discussed in the following section, and is corroborated by ~100% loss of Ca. This is consistent with Powder River Basin CCBs, which are also characterized by high concentrations of Ca and display similar leaching efficiencies.<sup>23,49,71</sup> The Boundary Dam, Shand, and Alberta CCBs showed similar leaching efficiencies as those from the Illinois and Appalachian Basins.<sup>71</sup> Despite Powder River Basin CCBs containing lower total REE abundances than Appalachian-derived CCBs, Taggart *et al.*<sup>23</sup> posited that higher extraction efficiency of Ca-rich ashes could compensate for the lower REE content. Therefore, Ca-rich ashes with moderate to high REE concentrations, such as those from Poplar River and the Powder River Basin, may be the most promising CCBs from which to extract REE because these ashes can be broken down more easily compared to those with higher silica contents.

The FAs had a greater leaching efficiency than the respective BAs which could be a function of their larger surface area: volume ratio allowing for increased contact area between the particle and acid. This has been shown previously, as Pan *et al.*<sup>80</sup> demonstrated that smaller size fractions released more REE during leaching. However, the difference in leaching efficiency between FAs and BAs could also be attributed to the mode of occurrence of the REE where the mineralogy of the coal could play a role in controlling the partitioning of the REE into the ashes, a possibility that requires further investigation. For the BAs, the Boundary Dam BA had the highest leaching efficiency for REE and the majority of the trace elements, whereas <10% of the metals were leached from the Alberta BAs. The Boundary Dam samples also had slightly higher leaching efficiency for REE and trace metals than those from the Shand plant, as did the samples from the higher temperature AB3 generator compared to the AB12 generator, indicating a potential boiler temperature control.

For all samples, excluding the Poplar River BA and Boundary Dam BA, the HREE were leached more effectively than the LREE. This was previously observed in acid leaching experiments from alkali-roasted CFA samples and was attributed to the HREE residing in Fe-rich minerals like hematite, goethite, and almandine, whereas the LREE were associated with Ti and/or aluminosilicate-rich minerals including allanite, rutile, and ilmenite.<sup>79</sup> Therefore, increased leaching of HREE relative to LREE is likely attributable to differences in mineralogy between the phases which host the LREE and HREE.

The results indicate that 3 M HCl can effectively leach REE from the Poplar River CCBs which are Ca-rich; however this method was not as effective for the Boundary Dam, Shand, or Alberta CCBs which have higher Si and lower Ca contents. Increasing the concentration of acid may not alleviate this

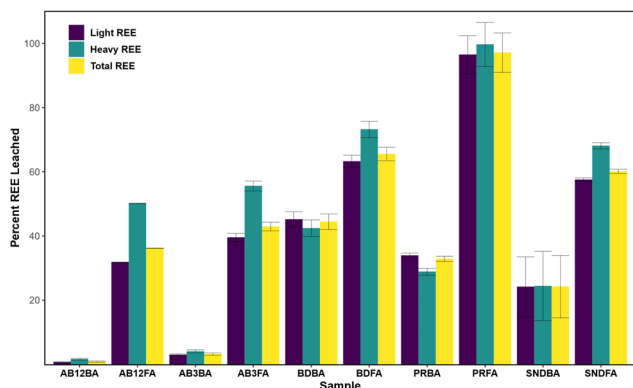


Fig. 2 Acid leaching results showing the percent of REE released following a 3 M HCl leach. Solid bars represent the average of duplicate analyses while the range of the concentrations between the duplicates are shown by the error bars.



issue: Cao *et al.*<sup>36</sup> found that the leaching efficiency improved as HCl concentration was increased up to 3 M; however, at higher concentrations, the increase in leaching efficiency was negligible which they attributed to the excess acid being unable to dissolve the REE in the glassy residual phase. Conversely, Mokoena *et al.*<sup>79</sup> postulated that excess  $H^+$  in solution could lead to the formation of silicic acid and subsequently a gel layer that would inhibit further dissolution. Instead, indirect leaching using an alkaline pre-treatment may be more appropriate for the CCBs from locations with high Si concentrations. King *et al.*<sup>71</sup> found that pre-treatment with NaOH at 85 °C prior to leaching with HCl significantly increased the overall leaching efficiency of Appalachian Basin-derived CCBs, while similar findings were described for CCBs from Sichuan, China.<sup>32</sup> Other studies have found that roasting the CCBs in the presence of Na compounds prior to an HCl leach also greatly increases the REE leaching efficiency.<sup>79,81</sup> Further investigations for the extraction potential of the Si-rich CCBs from Boundary Dam, Shand, and Alberta should therefore consider indirect leaching processes.

### Sequential extractions

Sequential extractions are a common quantitative method to elucidate the mode of occurrence of elements in geological samples. Results from the sequential extraction (Fig. 3) displays the percent of TREE present in each of the five fractions: (1) exchangeable; (2) acid soluble; (3) reducible; (4) oxidizable; and (5) residual. Sequential extraction results for the trace elements are presented in Fig. SI2.† The exchangeable phase did not host an appreciable amount of REE with all samples containing <0.1%, however it did host 24% of the Ca in the A3 FA and minor amounts of K, Ca, Sr, and Ba in each sample. REE in the acid soluble phase ranged from 0.33% in the A12BA to 9.3% in the Poplar River FA, with the highest abundance found in this sample being consistent with the acid leach experiments. In the FAs, 21–56% of the P resided in the acid soluble phase, as well as minor to trace amounts of Al, Si, K, Ca, Ti, V, Fe, Co, Ga, Sr, Zr, and Ba. The Poplar River FA also had the greatest proportion of REE in the reducible phase, likely associated with iron oxides, at 21.4%, as well as Ca, Al, V, and Co. Conversely, the Alberta

samples had the lowest amount of REE in the reducible phase. None of the REE were present in the oxidizable phase as all samples had concentrations below detection limits, however this phase did host small amounts of Al, Si, K, Ca, V, Rb, Sr, Ba, Fe, and Co in some samples. Overall, the REE were primarily hosted in the residual phase, ranging from over 98% in the Alberta BAs to 69% in the Poplar River FA, with only P, Ca, V, Sr, and Ba being below 80% in some samples. These findings are similar to previous studies which found that REE were primarily hosted in the residual phase of CCBs.<sup>22,49,61,82,83</sup>

Typical crystalline mineral phases present in CCBs can include quartz, mullite, hematite, magnetite, kaolinite, illite, periclase, anhydrite, lime, pyrite, calcite, and calcium-manganese oxides,<sup>34,44,55,84</sup> with the aluminosilicate minerals being the most abundant components in Class F fly ash.<sup>25</sup> SHRIMP-RG ion microprobe analysis of CCBs from the United States indicated that REE were mainly present in aluminosilicates, while acid leaching experiments on the same CCBs showed poor REE recovery in all samples except those from the Powder River Basin.<sup>23</sup> Given this, these studies concluded that the aluminosilicate phase was the major host of REE in CCBs. However, Kolker *et al.*<sup>25</sup> found that Ca-bearing and Fe-oxide phases could be important hosts of REE. Similarly, sequential extraction results for the Poplar River FA sample, which has lower  $SiO_2$  and higher  $Fe_2O_3$  and CaO concentrations than the other ashes considered here, suggest that the REE are distributed throughout different phases. This could indicate that the mineralogical REE host phase is distributed throughout the FA particle not just within the residual, glassy phase. However, this likely depends on the overall composition of the ash. Previous XANES analysis indicated that Y speciation of individual Y hotspots differs from the major form of Y observed at the bulk scale and that there could be multiple modes of occurrence of REE in CCBs.<sup>22</sup> Further high-precision analytical work, such as X-ray Absorption Fine Structure (XAFS), Micro X-ray Diffraction ( $\mu$ XRF), and/or tunnelling electron microscope – selected area electron diffraction (TEM-SAED) could assist in determining the precise host of the REE in CCBs, and additional work to determine the distribution of that host phase throughout the ash particle could be informative to the development of future extraction processes.

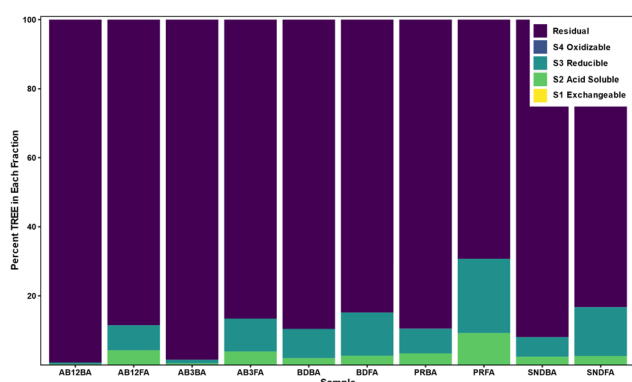


Fig. 3 Sequential extraction results indicating the percentage of REE present in each of the five sequential extraction phases: (1) exchangeable; (2) acid soluble; (3) reducible; (4) oxidizable; and (5) residual.

### Statistical analysis and machine learning

A dataset of CCB geochemistry from previous studies was compiled to compare the REE contents of CCBs from western Canada to those from around the world and to determine correlations between elements and reveal possible geochemical indicators of REE enrichment. The dataset compiled here is not intended to constitute a comprehensive review of global CCB chemistry, but rather provide a sample of published CCB data. Nd is highlighted in this section it is anticipated to experience the largest increase in demand as a result of the energy transition and TREE concentrations can be influenced by anomalous concentrations of less valuable, abundant elements such as La and Ce. Fig. 4A displays the Nd concentration by country and coal type. Kruskal-Wallis statistical testing performed in base R



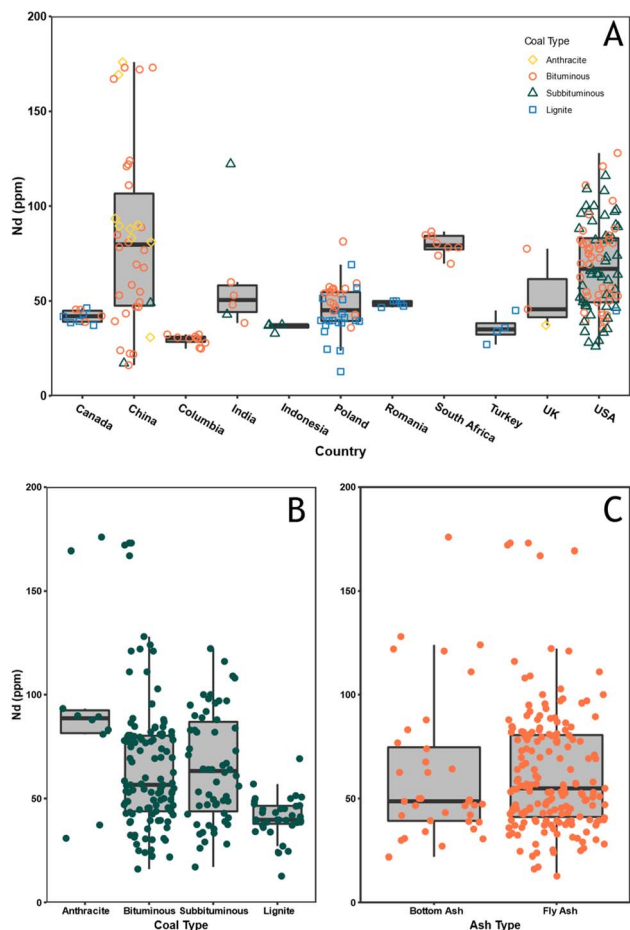


Fig. 4 A: Nd concentration by country and coal rank. B: Nd concentration by coal rank. C: Nd concentration between fly and bottom ashes.

indicates there are statistically significant differences in Nd abundances between countries since  $p < 0.05$ . A pairwise Wilcoxon rank sum test shows that the Canadian CCBs are statistically similar to ashes from India, Poland, Turkey, and the UK that were included here. The effect of coal rank on Nd concentrations were also assessed and is shown in Fig. 4B. The Wilcoxon rank sum test indicates that Nd concentrations in CCBs from bituminous and subbituminous coals are statistically similar, however this could be a result of the limited size of the dataset. Finally, the concentration of Nd in FA and BA were compared (Fig. 4C) and the Kruskal-Wallis test indicates that the concentrations in these fractions are statistically similar and could have a similar potential as a source of Nd and REE.

Geochemical data is considered compositional, such that the sum of the components theoretically sums to a whole (*i.e.* 1 or 100%).<sup>85</sup> As such, spurious correlations can occur, requiring transformation of the data prior to multivariate analysis.<sup>86</sup> Previous studies have applied log-ratio transformations to coal and coal ash data prior to multivariate analysis because it eliminates the “closure” problem.<sup>87,88</sup> Accordingly, a centred log-ratio (CLR) transformation<sup>85</sup> was applied to the data in Table S12† prior to correlation analysis, PCA, and cluster analysis

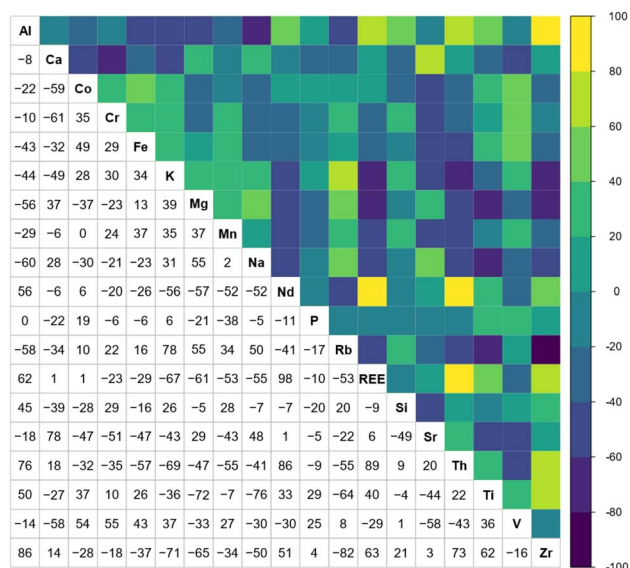


Fig. 5 Correlation matrix displaying the Pearson correlation coefficient for each element pair in the CLR transformed data.

using the compositions package<sup>89</sup> in R. Correlation coefficients can be used to determine the degree to which two variables are associated and has previously been applied in coal studies as an indirect method for assessing the mode of occurrence for trace elements.<sup>88,90</sup> The correlation matrix for the CLR transformed data (Fig. 5) shows that Nd, and REE as a group, have the highest correlation coefficients for Al, Ti, Th, and Zr.

Principal component analysis (PCA) and cluster analysis are unsupervised machine learning algorithms used in exploratory data analysis to reveal associations between elements and find structure within the dataset. PCA is a multivariate data analysis technique used to reduce the dimensionality of a dataset with multiple interrelated variables, while simultaneously retaining as much variation in the dataset as possible.<sup>91</sup> Similarly, cluster analysis can be used to partition multivariate observations into homogeneous groups based on similarities between variables.<sup>92</sup> Due to the close association of Nd and REE, Nd was used as a proxy for REE as a group in the PCA and cluster analysis. The PCA biplot is shown in Fig. 6, while the scree-plot and the variable contributions to the first and second principal components (PCs) are presented in Fig. S13 and S14.† Based on the PCA results, five PCs account for 85.9% of variance in the dataset. Sodium has the largest contribution to dimension one, while Ca and Th have the largest contributions to dimension two. Since the correlation coefficient of two variables is approximated by the cosine of the angle between two rays in a CLR-transformed biplot,<sup>93</sup> the PCA performed here indicates that Al, Th, Ti, and Zr are most correlated with Nd.

The cluster dendrogram for the hierarchical cluster analysis is shown in Fig. 7 and indicates Ti, Si, Zr, Al, and Th are closely related to Nd, and by extension REE. Taken together, the correlation analysis, PCA, and cluster analysis indicate that REE is most associated with incompatible elements (Th, Zr, and Ti), which is not unexpected given their geochemistry, where REE





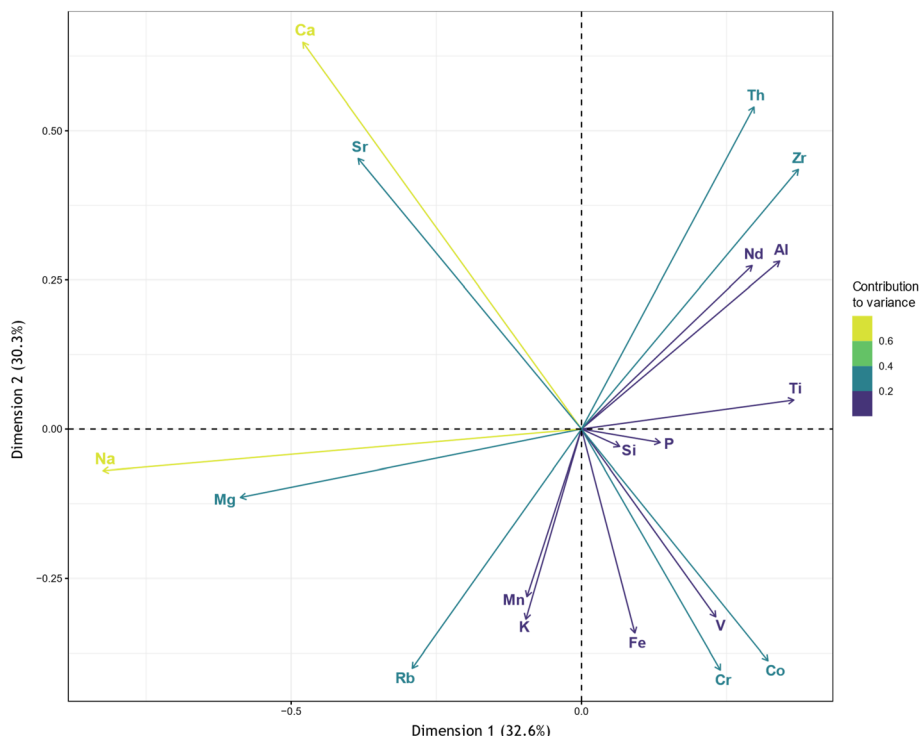


Fig. 6 PCA biplot of the CLR transformed data displaying dimensions 1 and 2.

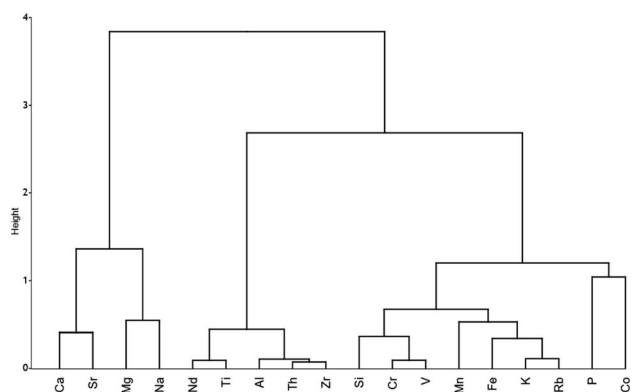


Fig. 7 Hierarchical cluster analysis for CLR transformed data.

are often delivered through an influx of detrital mineral phases in sedimentary environments.<sup>94</sup> One condition that should be met when applying statistical methods to coal analyses is that the dataset should be homogeneous, with samples coming from the sample stratigraphic horizon.<sup>95</sup> While this is not the case here and results should be taken with caution, this could be indicative of mineral host-phase associations of REE within coals.

#### Mode of occurrence of trace elements in CCBs

Constraining the mode of occurrence of elements in CCBs is important as this can dictate their binding environment and mineralogy which has implications for the recovery of valuable elements, such as REE. However, determining the mode of

occurrence of REE in coal ash may be difficult due to the complex matrix and composition of the particles. For instance, REE in CCBs are typically heterogeneously distributed among crystalline minerals, amorphous materials, and unburned carbon.<sup>70</sup> Both direct methods (laser ablation ICP-MS, electron microscopy, microprobe, and synchrotron spectroscopy) and indirect methods (statistical analyses, sequential extractions, acid leaches, and physical separations) can be used to reveal the mode of occurrence in coal and its ash. Common REE-bearing minerals in coals include phosphates, carbonates, isomorphic admixtures in minerals, and clays.<sup>70,96</sup> Previous REE speciation studies point towards two capture mechanisms for the incorporation of REE into the ashes: the first being incorporation of the individual REE-bearing mineral grain into Si–Al melts, and the second being direct incorporation of the REE into aluminosilicates during the melting process.<sup>70</sup>

Although correlation analysis, PCA, and cluster analysis are all indirect methods for determining the mode of occurrence of elements, they each indicate that Nd (and subsequently REE as a group) are closely associated with Al, Th, Ti, and Zr. The PCA and cluster analysis also indicate a lesser association of Nd with P and Si. Reviews on the mode of occurrence for these elements found that Al is typically associated with silicates, specifically clay minerals including kaolinite and mixed-layered clays; Th is mainly associated with aluminosilicates and occasionally monazite, zircons, and carbonates; Ti is associated with Ti-oxides or clays; and Zr is commonly associated with zircons.<sup>90,96,97</sup> REE-bearing mineral phases in coals include: (i) detrital minerals, such as zircon, monazite, apatite, and xenotime; (ii) authigenic minerals such as carbonates,



fluorocarbonates, and phosphates;<sup>96</sup> and (iii) clay minerals which can adsorb REE.<sup>97</sup> In low grade coals, there is evidence that Al, Th, Ti, and REE can also be associated with organic matter.<sup>96</sup> In some cases, such as the Fire Clay coals in the USA, volcanic ash-derived tonstein can be a significant source of REE.<sup>30</sup>

In agreement with findings from previous studies, REE in CCBs from Saskatchewan and Alberta primarily reside in the residual phase indicated by the sequential extractions. However, the Poplar River FA also had an appreciable REE component in the acid soluble and reducible phases indicating associations with carbonate and iron minerals. The acid leach data shows that several trace elements, including those shown to have associations with coal through the statistical analyses (Al, P, Ti, and Th), were also leached with the REE indicating a similar mode of occurrence.

The geochemical and statistical analysis indicate that REE are found with elements commonly associated with clay minerals. This could indicate a detrital source, rather than a fluid-driven source (*i.e.*, hydrothermal fluids, surface water) of REE into these coals and subsequently the ashes. This is further supported by their association with Zr, which is likely hosted in zircons, and is a common indicator of a detrital source. Since the REE are leached in similar proportions to Al, Ti, Th, and Zr from these samples in both the acid leach and sequential extractions, it is likely that the REE-bearing phase is distributed throughout the ash, consistent with the first model of REE incorporation. The key difference, however, is that this mineral phase is not only hosted in the Si–Al phase: there may be multiple REE host phases, similar to findings by Taggart *et al.* using synchrotron spectroscopy.<sup>22</sup> This alternative interpretation is most probable for the high-Ca Poplar River FA sample and stands in contrast to previous studies which posited that the REE are primarily hosted in the aluminosilicate glass phase. Past studies, however, investigated ashes which had a predominantly Si–Al composition. As such, it is possible that the REE were shown to be dominantly present in the aluminosilicates due to bias in analysis where primarily ashes with elevated SiO<sub>2</sub> were studied.

### Implications for REE extraction from CCBs

Rare earth element distribution throughout the ash and surface area both play important roles in potential REE recovery,<sup>98</sup> while in the broader economic sense, major element composition and overall volume of the ash are critical when assessing coal based REE resource evaluation.<sup>24</sup> REE concentrations in CCBs are typically lower than that of traditional REE ore deposits, and therefore the recovery of these elements is unlikely to be as profitable unless recovery is part of a comprehensive, zero-waste, product-centred, valorization scheme.<sup>52</sup> CCBs with moderate REE concentrations and simpler extraction processes may therefore be better candidates as a REE source than CCBs with higher REE concentrations that require more costly extraction processes.<sup>24</sup> Extracting REE from CCBs is advantageous because it requires far less energy and capital expenditure than traditional mining since the exploration and development of a mine and several of the most energy

intensive processing steps are eliminated. However, variations in ash geochemistry and mode of occurrence would require that suitable recovery methods be tailored to the specific characteristics of each fly ash.<sup>20</sup> Given these considerations, when assessing CCBs as a potential source of REE, the ease of extractability may be more important than the total REE content.<sup>23</sup>

Based on our results, the Poplar River fly ash is the most favourable target for recovery because it has among the highest REE concentrations out of the studied Canadian ashes and the metals can be acid leached with relative ease. This is similar to the CCBs from Powder River Basin-derived coals, and extraction processes optimized for Powder River ash could feasibly be applied to Poplar River ashes. Due to the higher SiO<sub>2</sub> content, the Boundary Dam, Shand, and Alberta ashes would require a pre-treatment, such as NaOH leaching to decompose the aluminosilicates prior to acid leaching, similar to CCBs from Appalachian Basin coals.

## Conclusions

Addressing the supply of critical elements, including REE, through the development of novel, sustainable sources will be of fundamental importance in the next 20 to 30 years as society transitions to a net-zero approach in an effort to combat climate change. A critical first step in this regard is characterizing novel sources, the mechanisms that concentrate critical minerals, and developing an understanding of how they may be sustainably extracted. This study is the first to assess the REE potential of CCBs from western Canada. The Poplar River FA and Boundary Dam BA had the highest concentrations of TREE and CREE. The Poplar River ashes had the greatest leaching efficiency which is likely a result of their composition as they are characterized by lower abundances of SiO<sub>2</sub> and higher abundances of CaO relative to the other ashes. The sequential extraction results demonstrated that the REE in all the studied ashes are primarily hosted in the residual phase, followed by the reducible and acid soluble phases. Statistical analyses indicated that the REE concentrations in Canadian CCBs are similar to those from India, Poland, Turkey, and the UK. Correlation analysis, PCA, and cluster analysis all showed that REE in CCBs are most associated with Al, Th, Ti, and Zr which indicates that REE are likely associated with clay minerals. The geochemical and statistical analysis suggest that the REE-hosting mineral could be distributed throughout the ash particle as opposed to hosted solely in the glassy aluminosilicate phase.

The assessment provided here indicates that the Poplar River FA has the best potential for recovery since the REE can be released through acid leaching without pre-treatment. Due to their geochemical similarities to CCBs from the Powder River Basin, a similar extraction process could be applied to the Poplar River FA. Conversely, the Boundary Dam, Shand, and Alberta samples would likely require pre-treatment, such as NaOH leaching to break down silicates prior to recovery. Although data is presented for the three coal-fired power stations in Saskatchewan, only one plant in Alberta was investigated, as such additional work may be necessary to determine the REE potential of Alberta CCBs since their chemistry can vary



on a plant-by-plant basis. Further future work should focus on elucidating the specific mineralogical host of the REE in CCBs to determine whether the REE are bound directly in aluminosilicates or if they are hosted in a specific mineralogical phase which is distributed throughout the ash. Results will then be used to inform the development of an extraction process which ideally should be easily modifiable to recover REE from CCBs of varying composition. Designing an efficient, low-cost extraction method is what will ultimately dictate the economic feasibility of REE extraction from CCBs at a given location.

Although coal-fired powerplants are mandated by the Government of Canada to cease operation by 2030, or be retrofitted with a carbon capture system, recovery of REE from their ashes could provide a near-term, domestic source, providing a stop-gap supply until traditional mining operations come online. Additionally, this could provide employment opportunities in communities which will be affected by the closure of coal mines and associated power plants. Overall, CCBs could be an important source of REE and could be a crucial component in the transition to clean energy sources.

## Author contributions

BAB: conceptualization, methodology, software, validation, formal analysis, investigation, data curation, writing – original draft, writing – review & editing, visualization. KRS: methodology, software, validation, investigation, data curation, writing – review & editing. DSA: validation, resources, writing – review & editing, supervision, funding acquisition. LJR: conceptualization, methodology, validation, resources, writing – review & editing, supervision, funding acquisition.

## Conflicts of interest

The authors declare there were no conflicts of interest in the creation of this study.

## Acknowledgements

This work was supported through the financial contributions of the Natural Science Engineering Research Council of Canada (NSERC) in the form of a Canada Graduate Scholarship (CGS-D; BAB) and Discovery Grants (LJR: RGPIN-2021-02523 and DSA: RGPIN-2020-05289), as well as the Saskatchewan Geological Survey (Saskatchewan Ministry of Energy and Resources) through a doctoral scholarship (BAB). The authors would like to thank SaskPower and the power generation company from Alberta for supplying fly and bottom ash samples for this study and Gavin Jensen of the Saskatchewan Geological Survey. The authors would like to acknowledge the two anonymous reviewers whose insights greatly improved the quality of this manuscript.

## References

- 1 V. Balaram, Rare earth elements: A review of applications, occurrence, exploration, analysis, recycling, and environmental impact, *Geosci. Front.*, 2019, **10**(4), 1285–1303.
- 2 S. M. Jowitt, Mineral economics of the rare-earth elements, *MRS Bull.*, 2022, **47**, 1–7.
- 3 Y. Fujita, S. K. McCall and D. Ginosar, Recycling rare earths: Perspectives and recent advances, *MRS Bull.*, 2022, **47**, 1–6.
- 4 D. Gielen and M. Lyons, *Critical Materials for the Energy Transition: Rare Earth Elements*, International Renewable Energy Agency, Abu Dhabi, 2022.
- 5 U.S. Geological Survey, *Mineral Commodity Summaries 2022*, U.S. Geological Survey, 2022, p. 202, DOI: [10.3133/mcs2022](https://doi.org/10.3133/mcs2022).
- 6 Research and Markets, *Investigation Report on the Chinese Rare Earth Market 2021-2025*, [https://www.researchandmarkets.com/reports/5331413/investigation-report-on-the-chinese-rare-earth?utm\\_source=CI&utm\\_medium=PressRelease&utm\\_code=f3gz66&utm\\_campaign=1248502+-+China+Rare+Earth+Market+Report+2019-2023%3a+China%27s+Rare+Earth+Ex.2021](https://www.researchandmarkets.com/reports/5331413/investigation-report-on-the-chinese-rare-earth?utm_source=CI&utm_medium=PressRelease&utm_code=f3gz66&utm_campaign=1248502+-+China+Rare+Earth+Market+Report+2019-2023%3a+China%27s+Rare+Earth+Ex.2021).
- 7 J. D. Wilson, Whatever happened to the rare earths weapon? Critical materials and international security in Asia, *Asian Secur.*, 2018, **14**(3), 358–373.
- 8 X. Yin, C. Martineau, I. Demers, N. Basiliko and N. J. Fenton, The potential environmental risks associated with the development of rare earth element production in Canada, *Environ. Rev.*, 2021, 1–79.
- 9 G. G. Zaimes, B. J. Hubler, S. Wang and V. Khanna, Environmental life cycle perspective on rare earth oxide production, *ACS Sustain. Chem. Eng.*, 2015, **3**(2), 237–244.
- 10 S. R. Golroudbary, I. Makarava, A. Kraslawski and E. Repo, Global environmental cost of using rare earth elements in green energy technologies, *Sci. Total Environ.*, 2022, **832**, 155022.
- 11 K. Binnemans, P. T. Jones, B. Blanpain, T. Van Gerven, Y. Yang, A. Walton, *et al.*, Recycling of rare earths: A critical review, *J. Clean. Prod.*, 2013, **51**, 1–22.
- 12 S. M. Jowitt, T. T. Werner, Z. Weng and G. M. Mudd, Recycling of the rare earth elements, *Curr. Opin. Green Sustain. Chem.*, 2018, **13**, 1–7.
- 13 R. León, F. Macías, C. R. Cánovas, R. Pérez-López, C. Ayora, J. M. Nieto, *et al.*, Mine waters as a secondary source of rare earth elements worldwide: the case of the Iberian Pyrite Belt, *J. Geochem. Explor.*, 2021, **224**, 106742.
- 14 M. Hermassi, M. Granados, C. Valderrama, C. Ayora and J. L. Cortina, Recovery of rare earth elements from acidic mine waters: An unknown secondary resource, *Sci. Total Environ.*, 2022, **810**, 152258.
- 15 C. Ayora, F. Macías, E. Torres, A. Lozano, S. Carrero, J. M. Nieto, *et al.*, Recovery of Rare Earth Elements and Yttrium from Passive-Remediation Systems of Acid Mine Drainage, *Environ. Sci. Technol.*, 2016, **50**(15), 8255–8262.
- 16 S. Costis, K. K. Mueller, L. Coudert, C. M. Neculita, N. Reynier and J.-F. Blais, Recovery potential of rare earth elements from mining and industrial residues: A review and cases studies, *J. Geochem. Explor.*, 2020, **221**, 106699.

1 V. Balaram, Rare earth elements: A review of applications, occurrence, exploration, analysis, recycling, and



- 17 B. Swain, Red mud: An environmental challenge but overlooked treasure for critical rare earth metals, *MRS Bull.*, 2022, **47**, 289–302.
- 18 K. P. Pramanik and L. D. F. I. Nghiem, Extraction of strategically important elements from brines: Constraints and opportunities, *Water Res.*, 2020, **168**, 115149.
- 19 Y. Smith, P. Kumar and J. McLennan, On the Extraction of Rare Earth Elements from Geothermal Brines, *Resources*, 2017, **6**(3), 39.
- 20 W. Franus, M. M. Wiatros-Motyka and M. Wdowin, Coal fly ash as a resource for rare earth elements, *Environ. Sci. Pollut. Res.*, 2015, **22**(12), 9464–9474.
- 21 R. S. Blissett, N. Smalley and N. A. Rowson, An investigation into six coal fly ashes from the United Kingdom and Poland to evaluate rare earth element content, *Fuel*, 2014, **119**, 236–239.
- 22 R. K. Taggart, N. A. Rivera, C. Levard, J. P. Ambrosi, D. Borschneck, J. C. Hower, *et al.*, Differences in bulk and microscale yttrium speciation in coal combustion fly ash, *Environ. Sci.: Process. Impacts*, 2018, **20**(10), 1390–1403.
- 23 R. K. Taggart, J. C. Hower, G. S. Dwyer and H. Hsu-Kim, Trends in the Rare Earth Element Content of U.S.-Based Coal Combustion Fly Ashes, *Environ. Sci. Technol.*, 2016, **50**(11), 5919–5926.
- 24 D. A. Bagdonas, A. J. Enriquez, K. A. Coddington, D. C. Finnoff, J. F. McLaughlin, M. D. Bazilian, *et al.*, Rare earth element resource evaluation of coal byproducts: A case study from the Powder River Basin, Wyoming, *Renew. Sustain. Energy Rev.*, 2022, **158**, 112148.
- 25 A. Kolker, C. Scott, J. C. Hower, J. A. Vazquez, C. L. Lopano and S. Dai, Distribution of rare earth elements in coal combustion fly ash, determined by SHRIMP-RG ion microprobe, *Int. J. Coal Geol.*, 2017, **184**, 1–10.
- 26 A. C. Santos, A. Guedes, D. French, A. Futuro and B. Valentim, Integrative Study Assessing Space and Time Variations with Emphasis on Rare Earth Element (REE) Distribution and Their Potential on Ashes from Commercial (Colombian) Coal, *Minerals*, 2022, **12**(2), 194.
- 27 J. Liu, S. Dai, X. He, J. C. Hower and T. Sakulpitakphon, Size-dependent variations in fly ash trace element chemistry: Examples from a Kentucky power plant and with emphasis on rare earth elements, *Energy Fuels*, 2017, **31**(1), 438–447.
- 28 B. A. Bishop, G. K. S. Jensen and L. J. Robbins, Rare Earth Element Abundances in Coal Combustion Byproducts of Saskatchewan, *Summary of Investigations – the Saskatchewan Geological Survey*, 2022, vol. 1, 2022–4.1, pp. 1–9.
- 29 Z. Huang, M. Fan and H. Tian, Rare earth elements of fly ash from Wyoming's Powder River Basin coal, *J. Rare Earths*, 2020, **38**(2), 219–226.
- 30 J. C. Hower, J. G. Groppo, K. R. Henke, M. M. Hood, C. F. Eble, R. Q. Honaker, *et al.*, Notes on the potential for the concentration of rare earth elements and yttrium in coal combustion fly ash, *Minerals*, 2015, **5**(2), 356–366.
- 31 C. N. Lange, I. M. C. Camargo, A. M. G. M. Figueiredo, L. Castro, M. B. A. Vasconcellos and R. B. Ticianelli, A Brazilian coal fly ash as a potential source of rare earth elements, *J. Radioanal. Nucl. Chem.*, 2017, **311**(2), 1235–1241.
- 32 Z. Wang, S. Dai, J. Zou, D. French and I. T. Graham, Rare earth elements and yttrium in coal ash from the Luzhou power plant in Sichuan, Southwest China: Concentration, characterization and optimized extraction, *Int. J. Coal Geol.*, 2019, **203**, 1–14.
- 33 J. Pan, C. Zhou, C. Liu, M. Tang, S. Cao, T. Hu, *et al.*, Modes of Occurrence of Rare Earth Elements in Coal Fly Ash: A Case Study, *Energy Fuels*, 2018, **32**(9), 9738–9743.
- 34 N. J. Wagner and A. Matiane, Rare earth elements in select Main Karoo Basin (South Africa) coal and coal ash samples, *Int. J. Coal Geol.*, 2018, **196**, 82–92.
- 35 M. C. Frank and S. L. Bend, Peat-forming history of the ancestral Souris mire (Palaeocene), Ravenscrag Formation, southern Saskatchewan, Canada, *Can. J. Earth Sci.*, 2004, **41**(3), 307–322.
- 36 S. Cao, C. Zhou, J. Pan, C. Liu, M. Tang, W. Ji, *et al.*, Study on Influence Factors of Leaching of Rare Earth Elements from Coal Fly Ash, *Energy Fuels*, 2018, **32**(7), 8000–8005.
- 37 K. von Gunten, B. Bishop, I. Plata Enriquez, M. S. Alam, P. Blanchard, L. J. Robbins, *et al.*, Colloidal transport mechanisms and sequestration of U, Ni, and As in meromictic mine pit lakes, *Geochim. Cosmochim. Acta*, 2019, **265**, 292–312.
- 38 A. Tessier, P. G. C. Campbell and M. Bisson, Sequential Extraction Procedure for the Speciation of Particulate Trace Metals, *Anal. Chem.*, 1979, **51**(7), 844–851.
- 39 Z. Adamczyk, J. Komorek, B. Bialecka, J. Nowak and A. Klupa, Assessment of the potential of polish fly ashes as a source of rare earth elements, *Ore Geol. Rev.*, 2020, **124**, 103638.
- 40 S. Dai, L. Zhao, S. Peng, C. L. Chou, X. Wang, Y. Zhang, *et al.*, Abundances and distribution of minerals and elements in high-alumina coal fly ash from the Jungar Power Plant, Inner Mongolia, China, *Int. J. Coal Geol.*, 2010, **81**(4), 320–332.
- 41 S. Dai, L. Zhao, J. C. Hower, M. N. Johnston, W. Song, P. Wang, *et al.*, Petrology, mineralogy, and chemistry of size-fractionated fly ash from the Jungar power plant, Inner Mongolia, China, with emphasis on the distribution of rare earth elements, *Energy Fuels*, 2014, **28**(2), 1502–1514.
- 42 M. B. Folgueras, M. Alonso and F. J. Fernández, Coal and sewage sludge ashes as sources of rare earth elements, *Fuel*, 2017, **192**, 128–139.
- 43 J. C. Hower, J. G. Groppo, H. Hsu-Kim and R. K. Taggart, Signatures of rare earth element distributions in fly ash derived from the combustion of Central Appalachian, Illinois, and Powder River basin coals, *Fuel*, 2021, **301**, 121048.
- 44 Z. Huang, M. Fan and H. Tian, Rare earth elements of fly ash from Wyoming's Powder River Basin coal, *J. Rare Earths*, 2020, **38**(2), 219–226.
- 45 A. İ. Karayığit, Ö. Yiğitler, S. İşerli, X. Querol, M. Mastalerz, R. G. Oskay, *et al.*, Mineralogy and Geochemistry of Feed Coals and Combustion Residues from Tunçbilek and Seyitömer Coal-Fired Power Plants in Western Turkey, *Coal*





- Combustion and Gasification Products*, 2019, vol. 11, 18–31, pp. 438–456.
- 46 C. Lanzerstorfer, Fly ash from coal combustion: Dependence of the concentration of various elements on the particle size, *Fuel*, 2018, **228**, 263–271, DOI: [10.1016/j.fuel.2018.04.136](https://doi.org/10.1016/j.fuel.2018.04.136).
  - 47 J. Li, X. Zhuang, X. Querol, O. Font, N. Moreno and J. Zhou, Environmental geochemistry of the feed coals and their combustion by-products from two coal-fired power plants in Xinjiang Province, Northwest China, *Fuel*, 2012, **95**, 446–456.
  - 48 Z. Li, X. Li, L. Zhang, S. Li, J. Chen, X. Feng, *et al.*, Partitioning of rare earth elements and yttrium (REY) in five coal-fired power plants in Guizhou, Southwest China, *J. Rare Earths*, 2020, **38**(11), 1257–1264.
  - 49 P. Liu, R. Huang and Y. Tang, Comprehensive Understandings of Rare Earth Element (REE) Speciation in Coal Fly Ashes and Implication for REE Extractability, *Environ. Sci. Technol.*, 2019, **53**(9), 5369–5377.
  - 50 Z. Ma, X. Shan and F. Cheng, Distribution Characteristics of Valuable Elements, Al, Li, and Ga, and Rare Earth Elements in Feed Coal, Fly Ash, and Bottom Ash from a 300 MW Circulating Fluidized Bed Boiler, *ACS Omega*, 2019, **4**(4), 6854–6863.
  - 51 S. Mondal, A. Ghar, A. K. Satpati, P. Sinharoy, D. K. Singh, J. N. Sharma, *et al.*, Recovery of rare earth elements from coal fly ash using TEHDGA impregnated resin, *Hydrometallurgy*, 2019, **185**, 93–101.
  - 52 J. Pan, C. Zhou, M. Tang, S. Cao, C. Liu, N. Zhang, *et al.*, Study on the modes of occurrence of rare earth elements in coal fly ash by statistics and a sequential chemical extraction procedure, *Fuel*, 2019, **237**, 555–565.
  - 53 P. Prihutami, A. Prasetya, W. B. Sediawan, H. T. B. M. Petrus and F. Anggara, Study on Rare Earth Elements Leaching from Magnetic Coal Fly Ash by Citric Acid, *J. Sustain. Metall.*, 2021, **7**(3), 1241–1253.
  - 54 W. Rosita, I. M. Bendiyasa, I. Perdana and F. Anggara, Sequential particle-size and magnetic separation for enrichment of rare-earth elements and yttrium in Indonesia coal fly ash, *J. Environ. Chem. Eng.*, 2020, **8**(1), 103575.
  - 55 B. K. Saikia, C. R. Ward, M. L. S. Oliveira, J. C. Hower, F. De Leao, M. N. Johnston, *et al.*, Geochemistry and nano-mineralogy of feed coals, mine overburden, and coal-derived fly ashes from Assam (North-east India): A multi-faceted analytical approach, *Int. J. Coal Geol.*, 2015, **137**, 19–37.
  - 56 L. F. O. Silva, A. Jasper, M. L. Andrade, C. H. Sampaio, S. Dai, X. Li, *et al.*, Applied investigation on the interaction of hazardous elements binding on ultrafine and nanoparticles in Chinese anthracite-derived fly ash, *Sci. Total Environ.*, 2012, **419**, 250–264.
  - 57 D. Smolka-Danielowska, Rare earth elements in fly ashes created during the coal burning process in certain coal-fired power plants operating in Poland - Upper Silesian Industrial Region, *J. Environ. Radioact.*, 2010, **101**(11), 965–968.
  - 58 E. Strzałkowska, Rare earth elements and other critical elements in the magnetic fraction of fly ash from several Polish power plants, *Int. J. Coal Geol.*, 2022, **258**, 104015.
  - 59 B. Valentim, A. T. Abagiu, L. Anghelescu, D. Flores, D. French, P. Gonçalves, *et al.*, Assessment of bottom ash landfilled at Ceplea Valley (Romania) as a source of rare earth elements, *Int. J. Coal Geol.*, 2019, **201**, 109–126.
  - 60 Q. Wei and W. Song, Mineralogical and Chemical Characteristics of Coal Ashes from Two High-Sulfur Coal-Fired Power Plants in Wuhai, Inner Mongolia, China, *Minerals*, 2020, **10**(323), 1–23.
  - 61 F. Xu, S. Qin, S. Li, J. Wang, D. Qi, Q. Lu, *et al.*, Distribution, occurrence mode, and extraction potential of critical elements in coal ashes of the Chongqing Power Plant, *J. Clean. Prod.*, 2022, **342**, 130910.
  - 62 S. Zhang, S. Dai, R. B. Finkelman, I. T. Graham, D. French, J. C. Hower, *et al.*, Leaching characteristics of alkaline coal combustion by-products: A case study from a coal-fired power plant, Hebei Province, China, *Fuel*, 2019, **255**, 115710.
  - 63 L. Zhao, S. Dai, R. B. Finkelman, D. French, I. T. Graham, Y. Yang, *et al.*, Leaching behavior of trace elements from fly ashes of five Chinese coal power plants, *Int. J. Coal Geol.*, 2020, **219**, 103381.
  - 64 J. C. Hower, J. G. Groppo, H. Hsu-kim and R. K. Taggart, Distribution of rare earth elements in fly ash derived from the combustion of Illinois Basin coals, *Fuel*, 2021, **289**, 119990.
  - 65 R Core Team, *R: A Language and Environment for Statistical Computing*, R Foundation for Statistical Computing, Vienna, Austria, 2020, URL <https://www.R-project.org/>.
  - 66 K. Wright, *Corrgram: Plot a Correlogram*. R Package Version 1.13, 2018, <https://CRAN.R-project.org/package=corrgram>.
  - 67 A. Kassambara and F. Mundt, *Factoextra: Extract and Visualize the Results of Multivariate Data Analyses*. R Package Version 1.0.7, 2020, <https://CRAN.R-project.org/package=factoextra>.
  - 68 S. Garnier, *Viridis: Default Color Maps from 'matplotlib'*. R Package Version 0.5.1, 2018, <https://CRAN.R-project.org/package=viridis>.
  - 69 V. V. Seredin and S. Dai, Coal deposits as potential alternative sources for lanthanides and yttrium, *Int. J. Coal Geol.*, 2012, **94**, 67–93.
  - 70 B. Fu, J. C. Hower, W. Zhang, G. Luo, H. Hu and H. Yao, A review of rare earth elements and yttrium in coal ash: content, modes of occurrences, combustion behavior, and extraction methods, *Prog. Energy Combust. Sci.*, 2022, **88**, 100954.
  - 71 J. F. King, R. K. Taggart, R. C. Smith, J. C. Hower and H. Hsu-Kim, Aqueous acid and alkaline extraction of rare earth elements from coal combustion ash, *Int. J. Coal Geol.*, 2018, **195**, 75–83.
  - 72 S. Dai, I. T. Graham and C. R. Ward, A review of anomalous rare earth elements and yttrium in coal, *Int. J. Coal Geol.*, 2016, **159**, 82–95.
  - 73 M. Bau and P. Dulski, Distribution of yttrium and rare-earth elements in the Penge and Kuruman iron-formations,



- Transvaal Supergroup, South Africa, *Precambrian Res.*, 1996, **79**, 37–55.
- 74 S. R. Taylor and S. M. McLennan, *The Continental Crust: its Composition and Evolution*, 1985.
- 75 R. Bolhar, B. S. Kamber, S. Moorbath, C. M. Fedo and M. J. Whitehouse, Characterisation of early Archaean chemical sediments by trace element signatures, *Earth Planet. Sci. Lett.*, 2004, **222**(1), 43–60.
- 76 D. S. Alibo and Y. Nozaki, Rare earth elements in seawater: Particle association, shale-normalization, and Ce oxidation, *Geochim. Cosmochim. Acta*, 1999, **63**(3–4), 363–372.
- 77 X. Wang, J. A. Barrat, G. Bayon, L. Chauvaud and D. Feng, Lanthanum anomalies as fingerprints of methanotrophy, *Geochem Perspect Lett.*, 2020, **14**, 26–30.
- 78 L. Bartoňová, J. Serenčíšová and B. Čech, Yttrium partitioning and associations in coal-combustion ashes prior to and after their leaching in HCl, *Fuel Process. Technol.*, 2018, **173**, 205–215.
- 79 B. K. Mokoena, L. S. Mokhahlane and S. Clarke, Effects of acid concentration on the recovery of rare earth elements from coal fly ash, *Int. J. Coal Geol.*, 2022, **259**, 104037.
- 80 J. Pan, T. Nie, B. Vaziri Hassas, M. Rezaee, Z. Wen and C. Zhou, Recovery of rare earth elements from coal fly ash by integrated physical separation and acid leaching, *Chemosphere*, 2020, **248**, 126112.
- 81 M. Tang, C. Zhou, N. Zhang, J. Pan, S. Cao, T. Hu, *et al.*, Extraction of rare earth elements from coal fly ash by alkali fusion–acid leaching: Mechanism analysis, *Int. J. Coal Prep. Util.*, 2019, 1–20.
- 82 S. Park, M. Kim, Y. Lim, J. Yu, S. Chen, S. W. Woo, *et al.*, Characterization of rare earth elements present in coal ash by sequential extraction, *J. Hazard. Mater.*, 2021, **402**, 123760.
- 83 T. Nie, C. Zhou, J. Pan, Z. Wen, F. Yang and R. Jia, Study on the Occurrence of Rare Earth Elements in Coal Refuse Based on Sequential Chemical Extraction and Pearson Correlation Analysis, *Min. Metall. Explor.*, 2022, **39**(2), 669–678.
- 84 N. Rivera, N. Kaur, D. Hesterberg, C. R. Ward, R. E. Austin and O. W. Duckworth, Chemical composition, speciation, and elemental associations in coal fly ash samples related to the kingston ash spill, *Energy Fuels*, 2015, **29**(2), 954–967.
- 85 J. Aitchison, *The Statistical Analysis of Compositional Data*, Chapman and Hall, London, 1986, p. 416.
- 86 V. Pawlowsky-Glahn and J. J. Egozcue, Compositional data and their analysis: An introduction, *Geol. Soc. Spec. Publ.*, 2006, **264**, 1–10.
- 87 N. J. Geboy, M. A. Engle and J. C. Hower, Whole-coal versus ash basis in coal geochemistry: A mathematical approach to consistent interpretations, *Int. J. Coal Geol.*, 2013, **113**, 41–49.
- 88 N. Xu, M. Peng, Q. Li and C. Xu, Towards consistent interpretations of coal geochemistry data on whole-coal versus ash bases through machine learning, *Minerals*, 2020, **10**(4), 1–19.
- 89 K. G. van den Boogaart, R. Tolosana-Delgado and M. Bren, *Compositions: Compositional Data Analysis. R Package Version 2.0-2*, 2021, <https://CRAN.Rproject.org/package=compositions>.
- 90 J. Wang, O. Yamada, T. Nakazato, Z. G. Zhang, Y. Suzuki and K. Sakanishi, Statistical analysis of the concentrations of trace elements in a wide diversity of coals and its implications for understanding elemental modes of occurrence, *Fuel*, 2008, **87**(10–11), 2211–2222.
- 91 I. T. Jolliffe, *Principal Component Analysis*, Springer, New York, NY, 2002.
- 92 M. Templ, P. Filzmoser and C. Reimann, Cluster analysis applied to regional geochemical data: Problems and possibilities, *J. Appl. Geochem.*, 2008, **23**(8), 2198–2213.
- 93 N. Otero, R. Tolosana-Delgado, A. Soler, V. Pawlowsky-Glahn and A. Canals, Relative vs. absolute statistical analysis of compositions: A comparative study of surface waters of a Mediterranean river, *Water Res.*, 2005, **39**(7), 1404–1414.
- 94 R. L. Linnen, I. M. Samson, A. E. Williams-Jones and A. R. Chakhmouradian, Geochemistry of the Rare-Earth Element, Nb, Ta, Hf, and Zr Deposits, *Treatise on Geochemistry*, Elsevier Ltd, 2nd edn, 2013, vol. 13, pp. 543–568.
- 95 G. Eskanazy, R. B. Finkelman and S. Chattarjee, Some considerations concerning the use of correlation coefficients and cluster analysis in interpreting coal geochemistry data, *Int. J. Coal Geol.*, 2010, **83**(4), 491–493.
- 96 S. Dai, R. B. Finkelman, D. French, J. C. Hower, I. T. Graham and F. Zhao, Modes of occurrence of elements in coal: A critical evaluation, *Earth-Sci. Rev.*, 2021, **222**, 103815.
- 97 R. B. Finkelman, C. A. Palmer and P. Wang, Quantification of the modes of occurrence of 42 elements in coal, *Int. J. Coal Geol.*, 2018, **185**, 138–160.
- 98 J. Hower, J. Groppo, P. Joshi, S. Dai, D. Moecher and M. Johnston, Location of Cerium in Coal-Combustion Fly Ashes: Implications for Recovery of Lanthanides, *Coal Combust Gasif Prod*, 2013, **5**(1), 73–78.

